
About empirical models predicting the missile perforation of concrete barriers

J. Baroth, L. Daudeville, Y. Malécot

*Université Joseph Fourier – Grenoble 1 / Grenoble INP / CNRS
3SR Lab, Grenoble, F 38041, France*

jbaroth@ujf-grenoble.fr

ABSTRACT. This paper deals with empirical formulae predicting the perforation of reinforced concrete barriers. These formulae are usually validated for hard impacts only. Consequently, on the one hand, a simple method is proposed in case of soft impacts. For various tests, experimental and model predictions of perforation show a good agreement. On the other hand, recent tests at the material scale show that the behaviour of concrete under high confinement does not depend on the unconfined compressive strength of concrete after 28 days, f_{c28} . Therefore analytical models based on f_{c28} need to be considered with caution.

RÉSUMÉ. Cet article se focalise sur les modèles analytiques de prévision de la perforation de voiles en béton armé sous impact. Ces modèles ne sont en général valables que pour des projectiles rigides. D'une part, une méthode simple de prévision de la perforation est alors proposée dans le cas d'impacts mous. Les formules qui en découlent permettent de prévoir la perforation de dalles impactées dans le cadre de plusieurs campagnes de tests. D'autre part, de récents tests à l'échelle du matériau montrent que le comportement du béton sous fort confinement ne dépend pas de la résistance en compression simple à 28 jours, f_{c28} . Par conséquent, les modèles analytiques pour lesquels le béton est complètement caractérisé par f_{c28} doivent être utilisés avec précaution.

KEY-WORDS: soft and hard impacts, reinforced concrete, perforation

MOTS-CLES: impacts durs et mous, béton armé, perforation

1. Introduction

Different approaches exist to assess the possible perforation of a barrier submitted to a missile impact: experimental, numerical and particularly empirical methods are used depending on materials and stiffness of both target and striker. (Eibl 1987) has defined soft and hard impacts. Li *et al.* (2005) and Buzaud *et al.* (2007) have presented and assessed the existing empirical formulae used for the perforation prediction of reinforced concrete (RC) targets in case of hard impacts, *i.e.* rigid projectiles compared to the concrete target. Mebarki *et al.* (2008) have carried out a similar study for steel targets.

Empirical formulae used for the design of reinforced concrete barriers submitted to missile impacts consist of ballistic limits in the case of hard impacts. Only one empirical formula found suits for soft impacts (CEB, 1988), *i.e.* rigid targets compared to the projectiles, under some conditions. Generally, the prediction of perforation in case of soft impacts is based upon the assumption that the deformation of the projectile is independent on the structural response of the target. This assumption allows evaluating the contact force due to the projectile (Riera 1968).

In a first section, this article presents empirical formulae for the perforation prediction of reinforced concrete targets under impacts, the range of variables over which the formulae were identified is given. In a second section, the balance of energy in case of soft impacts is examined. It allows, under some assumptions, the prediction of the ballistic limit (or limit velocity). In a third section, the relevance of the various presented models is evaluated on the basis of tests of soft impacts performed at Meppen in the 70's (Jonas *et al.*, 1979), (Nachtsheim *et al.*, 1982) and recently performed (Iris 2010), (Pontiroli *et al.*, 2011). The fourth section presents recent results showing that the unconfined compressive strength of concrete cylinders after 28 days of ageing, f_{c28} , should not be considered as the only material parameter characterizing the perforation resistance of concrete barriers submitted to impacts. Therefore, empirical formulae generally used for the design of impacted concrete structures must be used with caution.

2. Perforation prediction of reinforced concrete barriers

Only one analytical approach has been found in literature dealing with the prediction of concrete barriers under soft impacts (CEB 1988). This method is derived from load-time measurements of a 20 000 kg military aircraft impacting a reinforced concrete wall; it predicts perforation when the average dynamic load, applied by the missile, reaches the dynamic punching strength of the slab. From this study, the ballistic limit of cylindrical deformable projectiles, of mass M (kg), diameter d (m), impacting RC structures is deduced:

$$V_{CEB} = 50 \frac{(r_d f_{c,cube})^{1/6}}{M^{0.31}} \sqrt{T(3.14d + 7.85T)} \quad [1]$$

Where r_d (%) is the percentage of reinforcement, T (m) is the distance between the impact face and the rebar mesh ($T \approx$ thickness of the target). $f_{c,cube}$ is the characteristic compressive strength of concrete cubes after 28 days of ageing ($f_{c,cube} \approx 1.25 f_{c28}$).

Authors estimated this prediction with about 20 % precision, if following ranges of variables are satisfied, denoting Ag the aggregate size: $0.07 < T < 0.9$ m ; $0.66 < d/T < 1.3$; $25 < f_{c,cube} < 63$ MPa ; $0.05 < Ag/T < 0.07$; $0.22 < r_d < 1.26$ %.

Concerning hard impacts, among various formulae predicting perforation – see the state of the art (Li *et al.*, 2005) – Buzaud *et al.* (2007) have selected 8 formulae estimating the ballistic limit of cylindrical rigid projectiles, of mass M diameter d , impacting RC structures of thickness e . They propose to assess these formulae using a database of 151 tests. According to this analysis, the following formula [2] is well satisfied if its validity domain is *a priori* respected (Berriaud 1978).

$$V_1 = 1.3 \rho_c^{1/6} f_{c28}^{0.5} \left(\frac{de^2}{M} \right)^{2/3} \quad [2]$$

Formula [2] is supposed valid (with 10 % precision) for the following range of variables : $0.5 < d/e < 1.5$; $20 < V < 250$ m/s ; $30 < f_{c28} < 45$ MPa ; $150 < M_a < 250$ kg/m³ ; $0.5 < r_d < 0.8$ % ; $0.5 < M / \rho_c e^2 < 1.5$; $30 < M < 300$ kg ; $10 < d < 30$ cm ; $10 < e < 60$ cm, where M_a is the reinforcement density, ρ_c is the mass density.

Formula [2] was used for the design of the containment wall of French nuclear reactors. It was improved in order to extend its validity range, in particular concerning concrete strength, the reinforcement ratio and the projectile nose shape (Berriaud *et al.*, 1983):

$$V_2^2 = 1.89 f_{c28} \rho_c^{1/3} \left(\frac{de_p^2}{M} \right)^{4/3} \left(\frac{f_{c28}}{\sigma_0} \right)^{-1/2} N^2 \left(0.35 \left(\frac{M_a}{M_{a0}} \right)^\gamma + 0.65 \right)^2 \quad [3]$$

with $\sigma_0 = 36$ MPa, $M_{a0} = 200$ kg/m³, $N = 1$ and $N = 1.18$ for noses respectively flat, hemispheric then conic with angle α :

$$N = 3,24 - 6,01 \cdot 10^{-2} \alpha + 6,58 \cdot 10^{-4} \alpha^2 - 3,34 \cdot 10^{-6} \alpha^3 - 6,45 \cdot 10^{-9} \alpha^4 \quad [4]$$

The validity domain of [3] is *a priori*: $0.25 < d/e < 3.3$; $20 < V < 250$ m/s ; $15 < f_{c28} < 80$ MPa ; $0 < M_a < 300$ kg/m³.

Buzaud *et al.* (2007) concluded that formula [3] is the most precise among 8 formulae when they are applied to 151 tests including some of them out of their validity domain. We point out the high sensitivity of the ballistic limit regarding variations of the nose shape. The only material parameter characterizing concrete strength in [1]-[4] is f_{c28} , the unconfined compressive strength after 28 days of ageing. According to design codes, the calculation of concrete structures is usually based on f_{c28} , based on empirical relations, the majority of other characteristics can be deduced from f_{c28} (tensile strength f_t , Young's modulus E , etc.). Lots of concrete 3D constitutive models also use f_{c28} to scale the concrete 3D strength criterion. The section 4 examines the pertinence of using this unique parameter for characterizing concrete resistance to perforation.

Moreover, most formulae predicting perforation are not suited in case of soft impacts. In such cases, only numerical approaches (finite or discrete element methods) or non explicit analytical formulae seem available. The aim of the following section is to propose and to valid an explicit analytical formulation, to estimate ballistic limits. The difficulty is then to take into account the projectile deformation during the crash.

3. Prediction of concrete target perforation under soft impact

An explicit formulation is proposed. Then it is applied to results from various soft impact tests performed at Meppen in the 70's (Jonas *et al.*, 1979), (Nachtsheim *et al.* 1982) and recently performed (Iris, 2010), (Pontiroli *et al.*, 2011).

3.1. Analytical formulation of ballistic limits

3.1.1. Energetic formulation of the impact

Let us consider the energy W_p dissipated by the crushing of the projectile, as the mechanical work done by the constant crushing force F_p through the crushed length u of the projectile writes $W_p = F_p u$. That is equivalent to average the crushing force exerted by the projectile on the target during the crash. The idea of averaging this force was also found in (CEB 1988).

Let us denote $\Sigma = \frac{1}{2}M(V_0)^2$ the total kinetic energy at impact, where V_0 is the ballistic limit of the soft projectile. Let us suppose that this energy writes

$$\Sigma = W_p + \Sigma_p + W_c + \Sigma_c \quad [5]$$

The ballistic limit of the projectile, once it has been deformed, is denoted $V < V_0$, such that the kinetic energy of the projectile becomes $\Sigma_p = \frac{1}{2}MV^2$. The motion of

the target is characterized by the mechanical work $W_c = M_s a_s u_s$ and the kinetic energy $\Sigma_c = \frac{1}{2} M_s V_s^2$. If the motion of the target is supposed insignificant, a simple estimation of the ballistic limit V can be deduced from [5]:

$$V = \sqrt{V_0^2 + \frac{2F_p u}{M}} \quad [6]$$

3.1.2. Estimation of the crushing force of the projectile

The crushing force for hollow missiles is estimated by the following formula, based on Rankine's equation (Bignon *et al.*, 1980).

$$F_p = 2\pi e \left(\frac{\sqrt{2(1-\nu^2)}}{eE} + \frac{2}{d f_y} \right)^{-1} \quad [7]$$

where E is the Young's modulus (Pa), ν is the Poisson ratio, d is the projectile diameter (m), f_y is its limit strength (Pa), e is the thickness of the target (m).

In order to take into account the increase of the strength with the strain rate, the dynamic limit strength f_y^s is usually estimated, instead of f_y . Nevertheless, that is questionable in this work. Indeed, this effect of strain rate is maximal at the impact but decreases during the crash; therefore taking into account this effect and the proposed formulation should lead to overestimate crushing strengths and then ballistic limits. Moreover, the estimation of f_y^s does not seem precise. Applying the Johnson-Cook law (Johnson *et al.*, 1985) to a common steel ($f_y = 235$ MPa), Pontiroli *et al.*, (2011) predict a dynamic limit strength f_y^s greater than 480 MPa, whereas a method from (Jones 1989), used in (Moore *et al.*, 2011), leads to a value in the order of 460 MPa. The relevance of taking into account the strain rate effect in this work will be discussed in the following.

3.2. Application to soft impacts

Selected formulae predicting the perforation are applied to various tests, taking into account the crushing and the effect of the strain rate. These estimations are compared to test results. For all tests, projectiles are hollow metallic cylinders (soft steel, Poisson ratio $\nu = 0.3$, mass density $\rho_p = 7850$ kg/m³, Young's $E = 210$ GPa).

3.2.1. MEPPEN tests

Projectiles are steel cylinders ($d = 60$ cm, $f_y = 235$ MPa), whose lowest thickness is 7 mm over a length of 2.5 m and 10 mm over a length of 3 m. These parts can be crushed on a 6.5 x 6 m² slab of thickness 70 cm. The concrete slab is characterized

by a compressive strength f_c of 37.1 MPa and a density ρ_c of 2260 kg/m³ (Jonas *et al.*, 1979). Others characteristics of these tests are in table 1.

Reference / damage		II-2 / no perforation	II-5 / perforation limit	II-9 / perforation	
Tests	Mass M	1016 kg	974 kg	970 kg	
	Impact velocity V	172.2 m/s < V_0	234.8 m/s # V_0	235.8 m/s > V_0	
Soft impact models	[1]	231 m/s	232 m/s	232 m/s	
	no <i>strain rate effect</i>	[6] 7 mm	170 m/s	173 m/s	172 m/s
		[6] 7+10 mm	246 m/s	250 m/s	250 m/s
	<i>strain rate effect</i>	[6] 7 mm	214 m/s	217 m/s	217 m/s
		[6] 7+10 mm	326 m/s	333 m/s	334 m/s
Hard impact	Models [2-3]	121 m/s	122 m/s	121 m/s	

Table 1. Data concerning Meppen tests (Jonas *et al.*, 1979) ; measured initial velocities and estimated ballistic limits (m/s) (hard and soft impacts)

Table 1 presents velocities (m/s) measured and estimated for Meppen tests. For each test, the level of damage, the measured impact velocity and estimated ballistic limits are given. These limits are estimated regarding both hard and soft impacts.

In case of hard impact, formulae [2-3] approximate a ballistic limit of 121 m/s, with a relative difference less than 1 %. Therefore only the simplest formula [2] is used in the following. Table 1 shows that formulae [2-3] are not suited in case of these soft impacts, an initial velocity of 172 m/s being not enough to perforate.

In case of soft impact, table 1 provides five estimations. First, the formula [1] from [CEB 1988] is applied, its validity domain being verified. For the 3 tests, 232 m/s is a particularly good estimation of the ballistic limit. However, [CEB 1988] does not precise if Meppen tests results have been used to calibrate their approach. Then soft impacts are studied considering that lower and upper values of the dissipated energy during the crushing of the projectile are respectively given by $W_{p1} = 2.5 F_p$ and $W_{p2} = W_{p1} + 3 F_{p'}$, where F_p , $F_{p'}$ are the crushing forces given by [7], regarding respectively the 7 mm thick and the 10 mm thick parts of the projectile. These two parts are studied in table 1, which presents estimated ballistic limits, using formula [6] based on [2]. These velocities are also estimated taking into account the effect of strain rate (in italics), using the dynamic limit strength f_y^s instead of f_y in [7].

Obviously, [6] provides relevant estimations of lower and upper values of the ballistic limit, taking into account that all the first deformable (7 mm thick) part has been crushed but not all the other deformable (10 mm thick) part. Taking into

account the strain rate leads to higher estimations, in the same order, which seem logical but rather surestimated.

3.2.2. IRIS tests

Projectiles are metallic cylinders ($d = 25.4$ cm, $f_y = 340$ MPa, $M = 49,99$ kg), whose lowest thickness is 3 mm over a length of 1 m. These parts can be crushed on 15 cm thick slabs. Two tests are conducted with velocities equal to 110.15 and 111.56 m/s [Moore *et al.*, 2010]. The crushing force F_p for this part is around 540 kN. Taking into account the effect of strain rate, this force is found around 630 kN [Moore *et al.*, 2010].

Tests / damage	impact velocities (tests)	hard impact [2-3]	soft impact [1]	soft impact [6]	soft impact [6] with strain effect
1-2 /no perforation	110.1-111.6 m/s	85 m/s	152 m/s	170 m/s	180 m/s

Table 2. Measured and estimated velocities, in case of Iris tests (no perforation)

Table 2 presents velocities (m/s) measured and estimated for Iris tests. The level of damage and measured impact velocity and estimated ballistic limits are given. These limits are deduced in case of hard and soft impacts.

In case of hard impact, formulae [2-3] approximate the ballistic limit, with a relative difference less than 1 %. Therefore only the simplest formula [2] is used. Table 2 shows that formulae [2-3] are not suited in case of these soft impacts: 111 m/s are not enough to perforate, therefore 85 m/s is a bad estimation.

In case of soft impact, table 2 provides three estimations. First, the formula [1] from [CEB 1988] is applied, its validity domain being verified. For the test II-4, 152 m/s is not a bad estimation of the ballistic limit since 111 m/s are not enough to perforate. Then soft impacts are studied considering that the dissipated energy during the crushing of the projectile is given by $W_p = 1 F_p$ where F_p is the crushing force given by [7]. Table 2 presents estimated ballistic limits, using formula [6] based on [2], taking into account the effect of strain rate (in italics) or not.

Obviously, [1, 6] provide better estimations of the ballistic limit than [2-3]. Taking into account the strain rate leads to a higher estimation, in the same order.

3.2.3. VULCAIN tests

Projectiles are metallic cylinders ($d = 9,98$ cm, $f_y = 235$ MPa), whose lowest thickness is 1 mm over a length of 25 cm and of 2 mm over a length of 30 cm. These parts can potentially be crushed on 2.1×2.1 m² slabs of thickness e (6 and 7 cm).

Characteristics of tests are gathered in tables 3 and 4 (Pontiroli 2011). Tests 2 and 8 are presented in the last paper (Pontiroli *et al.*, 2011).

Parameters	Values	unit
ρ_c and ρ_p	2278 and 7850	kg/m ³
r_d ($e= 6$ and 7 cm)	1 and 1.2	%
f_c	28.6	MPa

Table 3. Common data to all tests (Pontiroli 2011)

	1	2	3	4	5	6	7	8	9
Reference	#22	#24	#30	#31	#35	#27	#43	#32	#34
M (kg)	6.166	5.2073	5.0916	5.0728	5.0594	4.9853	5.0509	5.0653	5.0596
e (m)	0.07	0.07	0.07	0.06	0.07	0.07	0.07	0.07	0.07
V (m/s)	135.5	107.5	92	89	73	93	80	70.2	68

Table 4. Specific data concerning each of nine Vulcain tests (Pontiroli, 2011)

Figure 1 presents ratios between measured velocities at impact and estimated ballistic limits. Moreover, figure 1 shows levels of damage for the 9 slabs tested (Pontiroli 2010). In case of perforation (tests 1 to 4), ratios must be less than 1. Instead, there is no perforation (ratio greater than 1). Test 6 is a particular case where all the concrete is perforated, but the projectile is just stopped by steel rods. Therefore the estimated ratio should be equal to one.

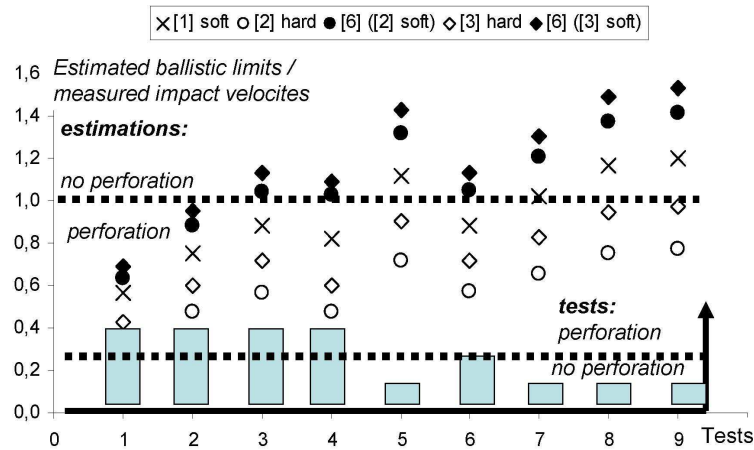
In case of hard impacts, formulae [2] and [3] are used. Figure 1 highlights insufficiency of classical formulae to distinguish perforation and no perforation. One notices for these tests that estimations [2] and [3] are quite different.

In case of soft impacts, three formulae are used.

First, formula [1] derived from CEB approach provides good estimations of perforation, excepted for tests 6 and 7. For these tests, there is no perforation and estimated ratios are respectively less than 1 and just equal to 1. Secondly, formula [6] is used, considering respectively [2] and [3]. The crushing force is estimated, taking into account only the first deformable (1 mm thick) part of the projectile, as it is verified in tests (Pontiroli 2010). Results are rather satisfactory, particularly if formula [6] is based on [3]. For tests 3 and 4, formula [6] underestimates ballistic limits, as estimated ratios are just equal to one; they should have been lower, as there is clearly perforation. For test 6, formula [6] provides a precise estimation of the ballistic limit, as the estimated ratio is just greater than one. For these tests,

estimations do not take into account the effect of strain rate. In this case, formula [6] would have been unable to predict which slab is perforated.

This section has presented a formula complementary to the only one available [CEB 1988]. Both have been able to predict perforation for various test results of soft impacts. The purpose of the next section is to present experimental results which show limits of formulae used in case of impacts, where stresses in the target reach high values.



Erreur ! Source du renvoi introuvable. *Velocities measured and estimated (hard and soft impacts), m/s*

4. Constitutive behaviour of concrete under high triaxial stress state

Gran and Frew (1997) have performed hard impact tests on concrete targets having an unconfined compressive strength of 43 MPa. The projectile was a 50 mm diameter steel sharp penetrator weighting 2.3 kg and was launched at 315 m/s. These authors have measured radial stresses at various depths and radii. They have shown that the maximum radial stress was about 400 MPa and, according to analytical calculations, the mean stress was of the order of 1 Gpa. *A priori*, in case of soft impacts, mean stress should also reach high values.

In order to analyze the behaviour of concrete under stresses of the order of 1 Gpa, triaxial tests on plain concretes have been performed, using a large capacity triaxial press. Stress levels over passing one GigaPascal have been reached (Gabet *et al.*, 2006, Gabet *et al.*, 2008, Vu *et al.*, 2009, Dupray *et al.*, 2009, Poinard *et al.*, 2010, Dupray *et al.*, 2010, Malécot *et al.*, 2010). In the following, complementary

results aim to highlight that f_{c28} is a very poor indicator of the high-pressure mechanical response of concrete.

4.1. Experimental set-up

4.1.1. Triaxial cell

The tests have been conducted with a high-capacity triaxial press that allows loading a cylindrical concrete specimen 7 cm in diameter and 14 cm long. This press is able to generate a maximum confining pressure of 0.85 GPa and an axial stress of 2.3 GPa. A displacement sensor located in the press is used to control the axial jack displacement, while a load sensor and pressure sensor placed inside the confinement cell display the stress state of the sample. The confining pressure and axial jack displacement are servo-controlled, which offers the possibility of creating several possible loading paths (Gabet *et al.*, 2006, Gabet *et al.*, 2008).

In the following, compressive stresses and contraction strains are assumed to be positive; σ_x is the principal axial stress, p the pressure inside the confining cell, $\sigma_m = (\sigma_x + 2p)/3$ the mean stress and $q = \sigma_x - p$ the principal stress difference (deviatoric stress). All tests have been conducted in following the same kind of loading path. The triaxial compression test begins with a hydrostatic test. Once the desired confinement has been reached, the specimen is then loaded axially while holding the confining pressure constant. Note that for most of the tests the maximum deviatoric stress reached value has not been imposed. It is a result of the test.

4.1.2. Concrete samples: f_{c28} and Sr

In order to study the effect of f_{c28} , from the composition of a reference ordinary concrete ($f_{c28} = 29$ MPa), two other concretes have been produced with f_{c28} equal to 21 MPa and 57 MPa, respectively. These three concretes have different water/cement ratio (W/C), but their aggregates skeletons are almost identical (see composition on table 5).

Concrete composition and mechanical properties	C57	C29	C21
0.5/8 "D" gravel (kg/m ³)	1000	1008	991
1,800 μ m "D" sand (kg/m ³)	832	838	824
CEM I 52.5 N PM ES CP2 cement (Vicat) (kg/m ³)	349	263	226
Water (kg/m ³)	136	169	181
Sikafluid Superplasticizer (kg/m ³)	4.5	0	0
W/C ratio	0.39	0.64	0.80
Density (kg/m ³)	2322	2278	2252
Average slump measured using the Abrams cone (cm)	7	6.9	14
Unconfined compression strength after 28 days f_{c28} (MPa)	57	29	21

Table 5. Compositions and mechanical properties of concretes C21, C29, C57.

Besides, to evaluate the effect of the saturation ratio S_r , tests have been conducted on dried, wet and saturated samples, for the C29 concrete. After some 4 months of conservation in water, the “dried” specimens are placed in a drying oven, at a temperature T of 50°C and relative humidity RH of 8 %, for a period lasting between 3 and 6 months. The saturation ratio of the “dried” concrete tested in this study is approximately 11 %. The “saturated” specimens are conserved in water between 6 and 10 months, after which they are wrapped in the multilayer membrane, just prior to the triaxial test. Lastly, the “wet” specimens are conserved in water and then a few days in the ambient laboratory atmosphere (a T value near 18°C and 40 % RH) during the instrumentation procedure (Vu *et al.*, 2009a).

Strain measurements are performed by use of an LVDT (Linear Variable Differential Transformer) axial sensor, along with one axial and two circumferential gauges. Given the porous nature of concrete, this high level of confinement has necessitated developing a multilayer protective membrane around the sample; this element is composed of 8 mm of latex and 2 mm of neoprene (Vu *et al.*, 2009b).

4.2. Test results

Figure 2 shows the results for the unconfined compression tests carried out on the four types of concrete samples. As it was expected, an increase in the Young's modulus E and ultimate stress of the concrete f_{c28} can be observed with a decrease in Water/Cement ratio of the concrete mixture. Figure 2 also reveals that the saturation ratio of the sample has a very slight influence in unconfined compression compare to the water/cement ratio.

Figure 3 shows the hydrostatic part of triaxial tests conducted at a confining pressure of 650 MPa. This figure reveals that beyond 400 MPa of confinement, the volumetric behaviour curves of dried concretes (C21, C29 or C57) run parallel, which suggests that the difference in incremental volumetric strains of these three concretes is significant only at low confinement levels. These phenomena are more obvious on Figure 4 which focuses on the hydrostatic behaviour of the same samples beyond a confining pressure of 400 MPa.

Figure 5 shows the deviatoric part of triaxial tests conducted at a confining pressure of 650 MPa. The results indicate that the deviatoric behaviour curves of dried concretes (C21, C29 or C57) practically overlap. The strength gap between these concretes is not anymore visible. The incremental behaviour of concretes becomes then independent from their unconfined compressive strength beyond a given confining pressure. On the contrary, the presence of free water in the sample seems to affect the volumetric stiffness only under high confinement. For a mean stress greater than around 200 MPa, the volumetric behavior of the wet concrete becomes stiffer than that of dried concrete (Figure 3). A relative difference of about 25 % between the volumetric strains of dried and saturated samples at a mean stress of 650 MPa can for example be noted. For these stress levels, the volumetric strains become significant compared to the initial air volume of the sample. The initially wet

samples thus trend toward a degree of humidity close to saturation. The pore pressure developing within the material rises and exerts a significant influence on the measured stress. The presence of free water in the sample also reduces a lot the strength capacity (Figure 5). The resistance capacity of the dried samples is clearly higher. As such, no peak deviatoric stress is reached in the tests conducted on dried concrete at these high confinements. These results may be explained by the cohesion loss of the cementitious matrix, which provides the concrete with behaviour of the non-cohesive granular material type. The increase in dried concrete shear strength with confining pressure is thus explained by the friction existing between stacking grains. Limitation of the same strength observed for saturated concrete is probably due to pore pressure, which develops similarly to what is found in undrained soils.

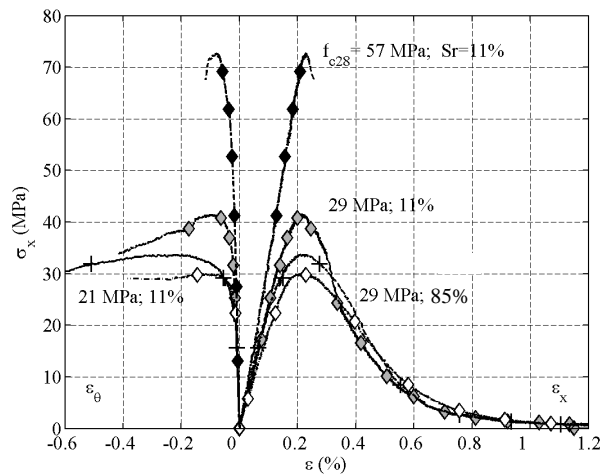


Figure 2. Axial stress σ_x vs. strain components ϵ_x and ϵ_θ for unconfined compression tests carried out on 4 types of 8 months aged concrete samples : C57 $f_{c28}=57$ MPa and $Sr=11$ % (\blacklozenge); C29-11% $f_{c28}=29$ MPa and $Sr=11$ % (grey diamond); C21 $f_{c28}=21$ MPa and $Sr=11$ % (\diamond); C29-85% $f_{c28}=29$ MPa and $Sr=85$ % (+).

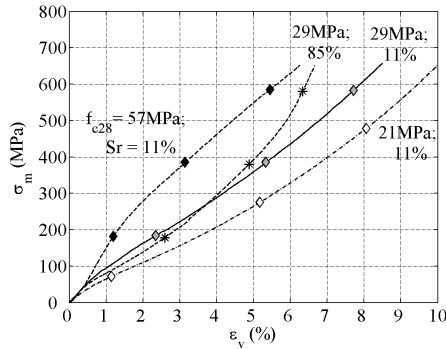


Figure 3. Mean stress σ_m vs. volumetric strain ϵ_v for the hydrostatic part of triaxial tests (confining pressure of 650 MPa) on four types of concrete samples: C57 $f_{c28}=57$ MPa and $Sr=11\%$ (\blacklozenge); C29-11% $f_{c28}=29$ MPa and $Sr=11\%$ (grey diamond); C21 $f_{c28}=21$ MPa and $Sr=11\%$ (\diamond); C29-85% $f_{c28}=29$ MPa and $Sr=85\%$ (*).

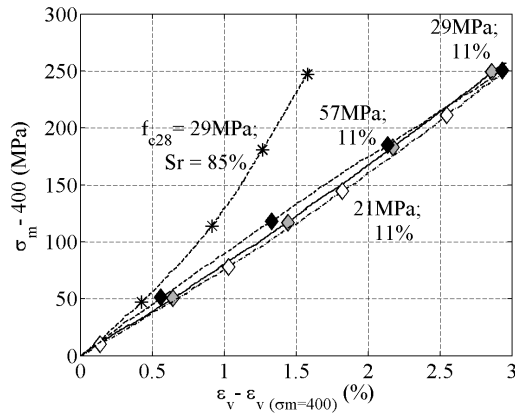


Figure 4. Mean stress σ_m vs. volumetric strain variation above 400 MPa $\Delta\epsilon_v = \epsilon_v - \epsilon_{v400MPa}$ for the hydrostatic part of triaxial tests conducted at a confining pressure of 650 MPa on four types of concrete samples: C57 $f_{c28}=57$ MPa and $Sr=11\%$ (\blacklozenge); C29-11% $f_{c28}=29$ MPa and $Sr=11\%$ (grey diamond); C21 $f_{c28}=21$ MPa and $Sr=11\%$ (\diamond); C29-85% $f_{c28}=29$ MPa and $Sr=85\%$ (*).

Figure 6 summarizes the strain limit state of concretes C21, C29 and C57, within the $(\sigma_m/f_{c28}, q/f_{c28})$ deviatoric plane for all tests performed. It can be observed that beyond a mean stress of around $5f_{c28}$, the loading capacity of dried concrete strongly increases in a quasi-linear manner with respect to the mean stress whereas the ones of wet or saturated concretes almost remain constant. Figure 6 also shows, on the one hand, that at low mean stress level (below $5f_{c28}$) all the concretes are following the same curve whatever Sr or f_{c28} values are. On the other hand, beyond this critical mean stress (over $5f_{c28}$), one can observe that the limit states are very scattered depending on Sr or f_{c28} values. This last point shows that f_{c28} is poorly link to the loading capacity of concrete under high confinement.

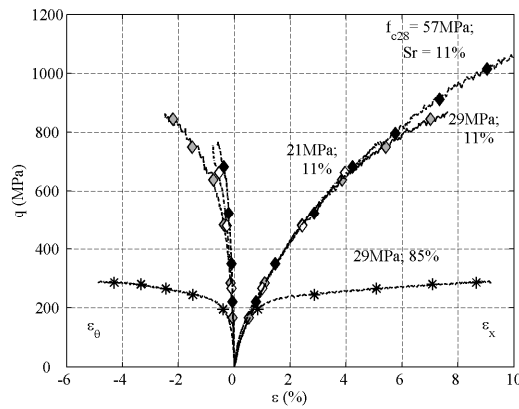


Figure 5. Stress deviator q vs. strain components ε_x and ε_θ for deviatoric part of triaxial tests conducted at a confining pressure of 650 MPa on four types of concrete samples: C57 $f_{c28}=57\text{MPa}$ and $Sr=11\%$ (\blacklozenge); C29-11% $f_{c28}=29\text{ MPa}$ and $Sr=11\%$ (grey diamond); C21 $f_{c28}=21\text{ MPa}$ and $Sr=11\%$ (\diamond); C29-85% $f_{c28}=29\text{ MPa}$ and $Sr=85\%$ (*).

Figure 7 shows the relative limit state of concretes C21, C57, C29-70%, C29-85 % and C29-100 % to that of the reference concrete C29-11% in the $(p, q/q_{C29-11\%})$ plane. $q_{C29-11\%}$ is the limit deviator obtained for the reference concrete C29-11% at an identical confining pressure. This presentation in terms of deviator relative to that of the reference concrete provides a better perception of the both the effect of the simple compressive strength at low confinement and the effect of the saturation ratio at high confinement. For low mean stress levels, the limit state of the concrete is heavily dependent on the cement matrix strength. This result was obviously the expected one. In contrast, the same figure also shows that this dependence of concrete limit state on f_{c28} decreases rapidly as mean stress rises. Beyond a critical confining pressure, the limit state curve actually becomes independent of f_{c28} .

Conversely, at a low level confining pressure, it is found that the limit states of the dried, wet and saturated samples all lie very close to one another (Figure 7). This result should come as no surprise since at such stress levels, concrete behaviour is governed by a still cohesive character. The presence of water in the sample does not exert therefore a very significant effect on the limit state. For higher confinement levels, the effect of water becomes predominant. The increase in peak deviatoric stress with respect to mean stress remains very low for the saturated samples. The shear strength of the dried concrete is then equal to 4 times the one of the saturated concrete for a confining pressure of 650 MPa, whereas their unconfined compressive strength is almost the same. Again, this phenomenon is likely explained by a pore pressure effect similar to that observed for an undrained granular material.

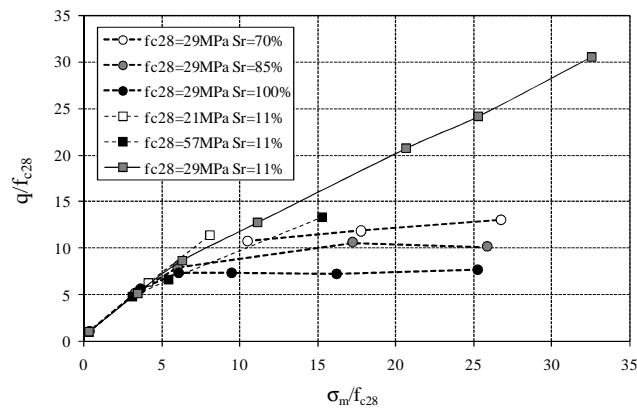


Figure 6. Limit states of concretes C21 ($Sr=11\%$), C29 ($Sr=11\%$, 70%, 85% or 100%) and C57 ($Sr=11\%$): Deviatoric stress q/f_{c28} vs. the mean stress σ_m/f_{c28} .

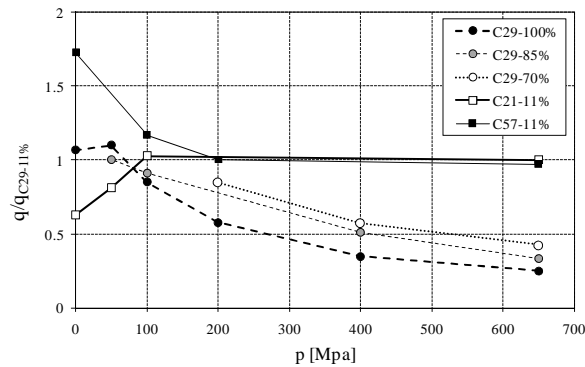


Figure 7. Relative limit states of concretes C21 ($Sr=11\%$), C29 ($Sr=70\%$, 85% or 100%) and C57 ($Sr=11\%$): Relative deviator $q/q_{C29-11\%}$ vs. the confining pressure p , where $q_{C29-11\%}$ is the deviatoric stress associated with the limit state of reference concrete C29 for $Sr=11\%$.

5. Conclusions

This paper has discussed the relevance of analytical models predicting the perforation of reinforced concrete targets.

In case of soft impacts, these formulae have to be developed. In this aim, a first empirical formula is derived from a past report [CEB 1988] and another simple method are proposed. For most tests, experimental and numerical predictions of perforation have shown a good agreement. Ongoing works consist to apply this last method to impacts on steel or composite targets, like tanks – that is not possible using the first approach –. As ballistic limits are proposed, it is also easy to deduce capacities of perforation, *i.e.* the maximal thickness to be perforated for given impact velocity.

In case of whatever hard or soft impacts, the test results provided in the second part of this article show that under high confinement, the concrete behaves like a non-cohesive granular stacking, on which the cement matrix strength of the fresh concrete no longer exerts any influence. It becomes insensitive with f_{c28} whereas the saturation ratio exerts a major influence, particularly on both the concrete strength capacity and the volumetric stiffness. According to this new result, the range of application of perforation formulae [1]-[4] presented in the previous section must be considered with caution.

From an application standpoint, on the one hand, these last results highlight the very small advantages to be gained by increasing the cement concentration in concretes for the purpose of raising their strength capacity to resist to extreme loadings. On the other hand, it seems necessary to evaluate and to take into account the saturation ratio to evaluate precisely the vulnerability under impact of massive concrete infrastructures. In the future, it will be necessary to evaluate the effect of the concrete porosity on the validity of these results. More specifically, do the above conclusions remain valid for very low porosity and/or high performance concretes?

6. Acknowledgements

The GIGA press has been installed in the 3SR Laboratory within the scope of a cooperative agreement with the CEA-Gramat. This research has been partially performed with the financial support of the French ministry of defense (DGA). Drs. Buzaud and Pontiroli (CEA-Gramat) are acknowledged for managing tests on slabs. The French Agency (ANR PGCU 2007) is also gratefully acknowledged.

7. References

- Berriaud C., Dulac J., Sokolovsky A., Labrot R., Gueraud R., Avet-Flancard R., « Local behaviour of reinforced concrete walls under missile impact », *Nuclear Engrg and Design*, vol. 45, n°2, 1978, p. 457-469.
- Berriaud C., Dulac J., Perrot J., Avet-Flancard R., « Impact on concrete: Synthesis of French Studies », *Proc. 7th SMiRT*, Chicago, USA, 1983, paper n°J8/2.
- Bignon P.G., Riera J.D., « Verification of methods of analysis for soft missile Impact problems », *Nuclear Engrg and Design*, vol. 60, n°3, 1980, p. 311-326.
- Buzaud E., Cazaubon C., Chauvel D., « Assessment of empirical formulae for local response of concrete structures to hard projectile impact », *Proc. CONSEC 07*, Tours, France, 2007, p. 1365-1372.
- CEB, « Concrete structures under impact and impulsive loading », Comité Euro-International du Béton, *Bulletin d'Information*, n°87, 1988, Lausanne, Switzerland.
- Dupray F, Malécot Y, Daudeville L, Buzaud E, « A mesoscopic model for the behaviour of concrete under high confinement », *International J. for Numerical and Analytical Methods in Geomechanics*, vol. 33, n°11, 2009, p. 1407-1423.
- Dupray F, Malécot Y, Daudeville L, « Experimental behaviour of high-performance concrete in confined tension », *Materials and Structures*, vol. 43, n°5, 2010, p. 699-707
- Eibl J., « Soft and hard Impact. Concrete for hazard protection », *Concrete Society*, Edinburgh, UK, 1987, p. 175-186.

- Gabet T, Vu X.H., Malécot Y, Daudeville L., « A new experimental technique for the analysis of concrete under high triaxial loading », *J. de Physique IV*, vol. 134, 2006, p. 635-644.
- Gabet T, Malécot Y, Daudeville L., « Triaxial behavior of concrete under high stresses: Influence of the loading path on compaction and limit states », *Cement and Concrete Research*, vol. 38, n°3, 2008, p. 403-412.
- Gran J. K., Frew D. J., « In-target radial stress measurements from penetration experiments into concrete by ogive-nose steel projectiles », *International J. of Impact Engrg*, vol. 19, n°8, 1997, p. 715-726.
- IRIS, « Benchmark on improving robustness assessment methodologies for structures impacted by missiles », NEA/IAGE Workshop, 13-15 December 2010. NEA Headquarters, France.
- Johnson G. R. and Cook W. H., « Fracture characteristics of three metals subjected to various strains, strain rates, temperatures and pressures », *Engrg Fracture Mechanics*, vol. 21, n°1, 1985, p. 31-48.
- Jonas W., Meschkat R., Riech H., Rüdiger E., « Experimental investigations to determine the kinetic ultimate bearing capacity of reinforced concrete slabs subject to deformable missiles », *Proc. 5th SMiRT*, Berlin, Germany, 1979, J8/3.
- Jones N., « Structural impact », Cambridge University Press, 1989.
- Li Q.M., Reid S.R., Wen H.M., Telford A.R., « Local impact effects of hard missiles on concrete targets », *International J. of Impact Engrg*, vol. 32, n°1-4, 2005, p. 224-284.
- Malécot Y, Daudeville L, Dupray F, Poinard C, Buzaud E, « Strength and damage of concrete under high triaxial loading », *European J. of Environmental and Civil Engrg*, vol. 14, n°6-7, 2010, p. 777-803.
- Mébarki A., Nguyen Q.B., Mercier F., Ami Saada R., Reimeringer M. « Reliability analysis of metallic targets under metallic rods impact: towards a simplified probabilistic approach », *J. of Loss Prevention in the Process Industries*, vol. 21, n°5, 2008, p. 518-527.
- Moore J. *et al.*, « IRIS 2010 International Benchmark, Improving robustness assessment methodologies for structures impacted by missiles, workshop proceedings », Working Group of components and structures, report of team ENSI / B&H, IRSN editor, 2010.
- Nachtsheim W., Stangenberg F., « Interpretation of results of Meppen slab tests – Comparison with parametric investigations », *Nuclear Engrg and Design*, vol. 75, n°2, 1982, p. 283-290.
- Poinard C, Malécot Y, Daudeville L, « Damage of concrete in a very high stress state: Experimental investigation », *Materials and Structures*, vol. 43, n°1-2, 2010, p. 15-29.

- Pontiroli C., Rouquand A., Mazars J., « Predicting concrete behaviour from quasi-static loading to hypervelocity impact. An overview of the PRM Model », *European J. of Environmental and Civil Engrg*, vol 14, n°6-7, 2010, p.703-727.
- Pontiroli C., Rouquand A., « Soft projectile impacts analysis on thin reinforced concrete slabs: tests, modeling, simulations », *European J. of Environmental and Civil Engrg*, 2011 (to appear).
- Riera J.D., « On the stress analysis of structures subjected to aircraft impact forces », *Nuclear Engrg and Design*, vol. 8, n° 4, 1968, p. 415-426.
- Vu X.H., Malécot Y, Daudeville L, Buzaud E., « Experimental analysis of concrete behavior under high confinement: Effect of the saturation ratio », *International J. of Solids and Structures*, vol. 46, n°5, 2009a, p. 1105-1120.
- Vu X.H., Malécot Y, Daudeville L., « Strain measurements on porous concrete samples for triaxial compression and extension tests under very high confinement », *J. of Strain Analysis for Engrg Design*, vol. 44, n°8, 2009b, p. 633-657.
- Vu X.H., Malécot Y, Daudeville L, Buzaud E, « Effect of the water/cement ratio on concrete behavior under extreme loading », *International J. for Numerical and Analytical Methods in Geomechanics*, vol. 33, n°17, 2009c, p. 1867-1888.